ISSN 1674-1056
http://cpb.iphy.ac.cn
http://iopscience.iop.org/cpb
中国物理 B
Chinese Physics
中国物理
Chinese Physics B

Structural and electrical properties of reactive magnetron sputtered yttrium-doped HfO_2 films

Yu Zhang(张昱), Jun Xu(徐军), Da-Yu Zhou(周大雨), Hang-Hang Wang(王行行), Wen-Qi Lu(陆文琪), Chi-Kyu Choi
Citation: Chin. Phys. B . 2018, 27(4): 048103. **doi:** 10.1088/1674-1056/27/4/048103

Journal homepage: http://cpb.iphy.ac.cn; http://iopscience.iop.org/cpb

What follows is a list of articles you may be interested in

Atomic-layer-deposited Al_2O_3 and HfO_2 on InAlAs: A comparative study of interfacial and electrical characteristics

Li-Fan Wu(武利翻), Yu-Ming Zhang(张玉明), Hong-Liang Lv(吕红亮), Yi-Men Zhang(张义门)
Chin. Phys. B . 2016, 25(10): 108101. **doi:** 10.1088/1674-1056/25/10/108101

Characterization of atomic-layer MoS_2 synthesized using a hot filament chemical vapor deposition method

Ying-Zi Peng(彭英姿), Yang Song(宋扬), Xiao-Qiang Xie(解晓强), Yuan Li(李源), Zheng-Hong Qian(钱正洪), Ru Bai(白茹)
Chin. Phys. B . 2016, 25(5): 058104. **doi:** 10.1088/1674-1056/25/5/058104

Modeling the reactive sputter deposition of Ti-doped VO_x thin films

Wang Tao, Yu He, Gu De-En, Guo Rui, Dong Xiang, Jiang Ya-Dong, Hu Rui-Lin
Chin. Phys. B . 2015, 24(6): 068104. **doi:** 10.1088/1674-1056/24/6/068104

Modeling and experiments of N-doped vanadium oxide prepared by a reactive sputtering process

Wang Tao, Yu He, Dong Xiang, Jiang Ya-Dong, Wu Rui-Lin
Chin. Phys. B . 2015, 24(3): 038102. **doi:** 10.1088/1674-1056/24/3/038102

Investigation of 4H–SiC metal–insulation–semiconductor structure with Al_2O_3/SiO_2 stacked dielectric

Tang Xiao-Yan, Song Qing-Wen, Zhang Yu-Ming, Zhang Yi-Men, Jia Ren-Xu, Lü Hong-Liang, Wang Yue-Hu
Chin. Phys. B . 2012, 21(8): 087701. **doi:** 10.1088/1674-1056/21/8/087701

Structural and electrical properties of reactive magnetron sputtered yttrium-doped HfO_2 films*

Yu Zhang(张昱)[1], Jun Xu(徐军)[1,†], Da-Yu Zhou(周大雨)[2], Hang-Hang Wang(王行行)[1], Wen-Qi Lu(陆文琪)[1], and Chi-Kyu Choi[3]

[1] *Key Laboratory of Materials Modification by Laser, Ion and Electron Beams, Ministry of Education, School of Physics, Dalian University of Technology, Dalian* 116024, *China*

[2] *School of Materials Science and Engineering, Dalian University of Technology, Dalian* 116024, *China*

[3] *Department of Physics, Jeju National University, Jeju* 63243, *Korea*

(Received 1 December 2017; revised manuscript received 12 January 2018; published online 10 March 2018)

Hafnium oxide thin films doped with different concentrations of yttrium are prepared on Si (100) substrates at room temperature using a reactive magnetron sputtering system. The effects of Y content on the bonding structure, crystallographic structure, and electrical properties of Y-doped HfO_2 films are investigated. The x-ray photoelectron spectrum (XPS) indicates that the core level peak positions of Hf 4f and O 1s shift toward lower energy due to the structure change after Y doping. The depth profiling of XPS shows that the surface of the film is completely oxidized while the oxygen deficiency emerges after the stripping depths have increased. The x-ray diffraction and high resolution transmission electron microscopy (HRTEM) analyses reveal the evolution from monoclinic HfO_2 phase towards stabilized cubic HfO_2 phase and the preferred orientation of (111) appears with increasing Y content, while pure HfO_2 shows the monoclinic phase only. The leakage current and permittivity are determined as a function of the Y content. The best combination of low leakage current of 10^{-7} A/cm^2 at 1 V and a highest permittivity value of 29 is achieved when the doping ratio of Y increases to 9 mol%. A correlation among Y content, phase evolution and electrical properties of Y-doped HfO_2 ultra-thin film is investigated.

Keywords: Y-doped HfO_2, ultra-thin film, high-k, x-ray photoelectron spectrum

PACS: 81.15.Cd, 77.55.df, 68.55.–a, 82.80.Pv **DOI:** 10.1088/1674-1056/27/4/048103

1. Introduction

In order to achieve the progressive down-scaling process of Si-based microelectronics devices, high-k dielectric materials including HfO_2, Al_2O_3, TiO_2, ZrO_2, CeO_2, Y_2O_3, and La_2O_3 can be used as a substitution for conventional SiO_2 gate oxide films to reduce the leakage currents and power consumptions.[1–4] Among the possible candidates, HfO_2 is one of the most attractive dielectrics due to its superior properties such as reasonable band gap offset with silicon, high dielectric constant, and thermodynamic stability in contact with Si.[5–7] In the meantime, HfO_2 has also been used as thermal protective coating, passivation layer, gas sensor, antireflection coating, and even used in teeth prosthetics.[8–11]

Hafnium oxide exhibits many polymorphic modifications. Under standard conditions, HfO_2 has a stable monoclinic crystalline phase (space group $P2_1/c$). The monoclinic HfO_2 transforms into a tetragonal phase (space group $P4_2/nmc$) when the temperature increases to 1700 °C, further heating up to 2600 °C leads to a transformation of HfO_2 into cubic phase (structural form of fluorite, space group $Fm3m$). It has been predicted from first-principles study that HfO_2 exhibits higher permittivity in the cubic ($\kappa \approx 27$) or in the tetragonal ($\kappa \approx 70$) phase than in the monoclinic phase ($\kappa \approx 17$).[12–14] As the permittivity of HfO_2 strongly depends on its crystallographic phase, it is desirable to prepare HfO_2 in the cubic or tetragonal form at lower temperature, which can be achieved by incorporating a certain amount of other elements into the HfO_2 film. So far, HfO_2 has been doped with Si, Ge, Mg, Y, Sr, Dy, Er, Gd, Sc, Ce, and Al.[15–21] Among these, Y-doped HfO_2 has been widely investigated because Y_2O_3 crystallizes into a body-centered-cubic structure, which has some resemblance to cubic hafnia. The substitution by Y ions results in the modification of the crystal symmetry from a stable monoclinic phase to high-symmetry cubic phase.[22,23]

In this work, HfO_2 thin films doped with yttrium are prepared on silicon by medium frequency reactive magnetron co-sputter deposition employing Y and Hf targets. The effects of Y content on the elemental chemical states, microstructures, and electrical properties of Y-doped HfO_2 films are investigated in detail and the results are presented and discussed.

2. Experiment

The yttrium-doped HfO_2 dielectric layer was deposited on p-Si (100) substrate by reactive magnetron sputtering in a

*Project supported by the National Natural Science Foundation of China (Grant Nos. 51272034 and 51672032) and the Fundamental Research Funds for the Central Universities, China (Grant No. DUT17ZD211).

†Corresponding author. E-mail: xujun@dlut.edu.cn

© 2018 Chinese Physical Society and IOP Publishing Ltd

designated oxide deposition chamber. There were three sputter sources in this vacuum chamber: two Hf (99.99%) sputter targets were arranged horizontally (50 mm apart from each other) and one Y (99.99%) sputter target was located above the facing targets. The substrates were cleaned by a standard RCA technique to remove organic and metallic contaminants from the wafer surfaces, then the native silicon oxide layers on the surfaces were removed by being immersed in HF solution (HF:H_2O = 1:10) for 5 min. All depositions were performed at room temperature at the constant working gas pressure of 7×10^{-4} 1.3 Pa, and the Ar and O_2 flow rate were both maintained at 40 sccm. The high resolution transmission electron microscopy (HRTEM) result showed that the thickness of the Y-doped HfO_2 layer was about 10 nm. To vary the yttrium content between samples, the Hf source power was kept at 100 W while the Y source power was varied from 30 W to 75 W. After sputtering, crystallization was induced by rapid thermal processing (RTP) in nitrogen ambient for 40 s at 850 °C. To form a metal–insulator–semiconductor (MIS) structure for further characterizing the electrical properties, 150-nm thick TiN circular probing pads (0.1 μm) were deposited onto the Y-doped HfO_2 layer using DC reactive magnetron sputtering deposition through a metallic mask.

The x-ray photoelectron spectroscopy (XPS) was adopted to determine the composition and the chemical states of the elements in the films. The adventitious C 1s peak at 284.8 eV was used to calibrate the binding energy measured from the surface layer to 3-nm deep, and the Si^0 $2p_{3/2}$ peak at 99.4 eV was used to calibrate the binding energy measured form 9.0 nm to 18 nm deep. The x-ray diffraction (XRD) was carried out to investigate crystalline structure and phase transformation changing with doping content. The HRTEM was used to study in depth the nanocrystalline HfO_2 films with and without Y doping. The contrasts of HRTEM images were enhanced by fast Fourier transform (FFT) using the software DigiralMicrograph (Gatan, USA). In order to characterize the electrical properties of Y-doped HfO_2 films, we measured the current–voltage (I–V) and dielectric constant characteristics using a Mutliferroic 100 V Test System (RT66B, Radiant Technologies, Inc., USA).

3. Results and discussion

3.1. XPS results analysis

The compositions and chemical states of the elements in Y-doped HfO_2 films are measured using XPS. The spectra are taken after etching the surfaces of the films by Ar^+ for 30 s to remove surface contaminations. The actual content values of Hf and Y in the films varying with Y target power are represented in Fig. 1. It is found that the concentrations of Hf in films decline with the increasing of power of the Y target. The reduction of Hf content indicates that yttrium as a substitutional atom successfully enters into the HfO_2 lattice structure, making some of the Hf–O–Hf bonds be replaced by Hf–O–Y.

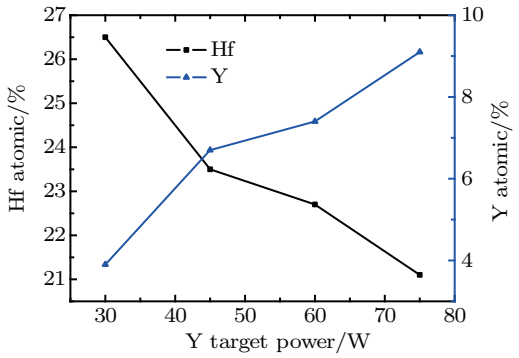


Fig. 1. (color online) XPS measured content of Y and Hf versus Y target power in the films.

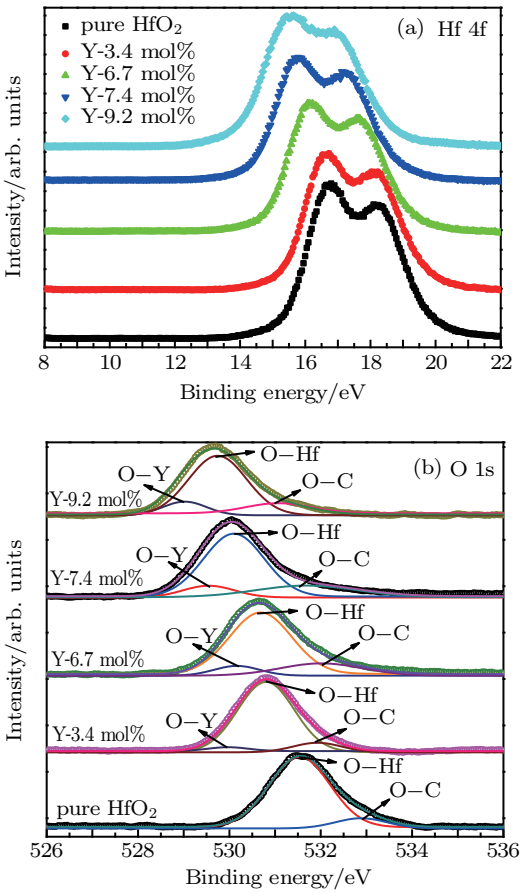


Fig. 2. (color online) XPS spectra for (a) Hf 4f core levels and (b) O 1s core levels taken from five different samples.

Figure 2 shows the XPS spectra of Hf 4f and O 1s of Y-doped HfO_2 films. It can be seen that the positions of peaks for both Hf 4f and O 1s shift to lower binding energy as yttrium content increases. Binding energies for Hf 4f core levels of the samples doped with different amounts of Y are shown in Fig. 2(a). For the sample without doping, two peaks at 16.74 eV and 18.34 eV are assigned to Hf $4f_{7/2}$ and Hf $4f_{5/2}$, respectively, and the spin-orbit splitting is 1.6 eV. When the Y doping concentration increases to 9.2 mol%, the positions of peaks shift to 15.45 eV and 17.05 eV, respectively. The shift of

Hf 4f core level peak position indicates that the incorporation of Y makes some of the Hf–O–Hf bond replaced by Hf–O–Y. Figure 2(b) shows the O 1s XPSs for these samples, all spectra are deconvoluted using the Lorentzian–Gaussian function. There are three peaks attributed to O–Y, O–Hf, and O–Si respectively. With the increasing of the content of Y, the O–Y component increases obviously and the O 1s peak shifts to a low-binding energy. The difference in electronegativity between Hf (1.30) and the additive (1.22 for Y) is responsible for the shift of O 1s peak. The incorporation of a lower electronegativity element can change the interaction between the atoms and make the core level of the element shift to lower binding energy.[24]

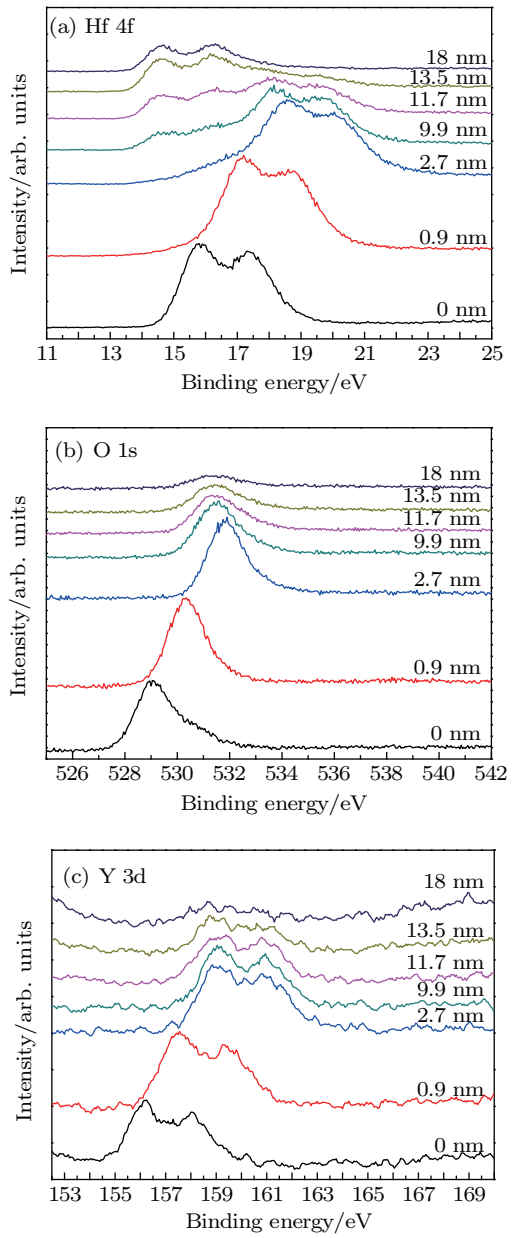


Fig. 3. (color online) XPS depth profiles for the Y-doped HfO_2 films of (a) Hf 4f, (b) O 1s, and (c) Y 3d core-level spectrum with seven stripping depths.

In order to clarify the interfacial chemical state more clearly, the depth profiles of the Y-doped HfO_2 film (Y-3.4 mol%) are investigated after different sputtering steps. Figure 3(a) shows Hf 4f core-level spectra with seven layers of stripping depths. Each surface layer presents a typical double-peak shape with the peak positions of 15.8 eV and 17.3 eV respectively, which is an indication of the forming of complete oxidation of Hf–O bonds. With the striping depths increasing to 2.7 nm, the feature peak shifts to the high-energy side. The peaks located at 18.6 eV and 20.1 eV represent the feature of Hf-rich HfO_2 film, which means that an oxygen deficiency has emerged. This oxygen deficiency in the bulk film might be caused by the preferred sputtering effect of Ar ion stripping during the XPS analysis procedure. The peak energy shift should be due to the Hf–O bond in the vicinity of Hf or Hf, Hf–O bond.[25] This explanation is further confirmed with the O 1s XPS spectra in Fig. 3(b). For the surface layer, the O 1s peak is located around 529 eV, indicating that the oxygen is in the form of Hf–O bonding. However, when the striping depth increases to 2.7 nm, the feature peak shifts to a higher energy side (at around 532 eV). These observations indicate that the total number of the Hf–O bonds decreases after ion sputtering.[26] As depth profiles are close to the Si substrate the Hf 4f doublet peak becomes weaker and ultimately disappears. At the same time the new peaks at 14.4 eV and 15.9 eV become detectable in the spectra, which were previously associated with the Hf–Si bond. Finally, the peak positions of Hf 4f change totally into Hf–Si after the stripping depth has reached to 18 nm. In the Y 3d core level spectra for different layers of stripping depths shown in Fig. 3(c), Y $3d_{3/2}$ and Y $3d_{5/2}$ doublet positions are observed at 158.2 eV and 156.2 eV for the surface layer, respectively, indicating the existence of a pure, well-oxidized Y–O bond. After ion sputtering, the Y 3d doublet position shifts about 2.8 eV to a higher binding energy. This could be attributed to increasing the number of the Y–O bonds in the film. There is no Y–Si bond that can be found at the Y-doped HfO_2/Si interface.

3.2. Phase identification

The phase stabilization effect of yttrium is investigated as a function of Y content with 10-nm thick Y-doped film. Figure 4 shows θ–2θ XRD patterns measured from Y-doped HfO_2 films. The structural phase difference between Y-doped and pure HfO_2 films is clearly observed by considering the diffraction angles of the peaks, only two peaks around 28.5° and 31.6° in pure HfO_2 can be seen, which are attributed to the monoclinic phase ($P2_1/c$). As the content of Y increases to 3.4 mol%, the crystalline phase emerges with three peaks around 30.7°, 51.0°, and 60.4°, which are attributed to (111), (022), and (113) planes of the HfO_2 cubic phase ($Fm3m$), while the m-phase is still existent, indicating the presence of a mixture of monoclinic HfO_2 and a higher symmetric HfO_2

phase. It is evident from the XRD plots that the peak intensities at 28.5° and 31.6° which belong to the monoclinic phase decline with the increasing of Y content, and no monoclinic phase is detected when the doping ratio of Y increases to 7.4 mol%. The film with a Y content of 7.4 mol% clearly crystallizes into a single cubic HfO_2 phase, and the stabilization of a purely cubic phase occurs between 6.7 mol% and 7.4 mol% for Y-doped thin films in our work. Furthermore, the intensity of the peak at 30.7°, which corresponds to the diffraction from (111) planes of the cubic phase, increase with increasing Y content. This is indicative of an increase in the preferred orientation of the film along (111) and a higher degree of crystallinity as a function of Y content. The ionic radius of Y is larger than that of Hf, which requires the elongation of the bonds with nearby O atoms. Compared with monoclinic and tetragonal phases, the cubic phase contains a longer Hf–O bond length, hence, the cubic phase is favored by the oversized Y doping.[27] A peak belonging to the Y_2O_3 phase is not detected from any of the samples, which means that yttrium has been successfully doped into the HfO_2 matrix.

Figure 5 shows the cross-sectional HRTEM images of HfO_2 films without (a) and with (b) Y doping. In Fig. 5(a), the inset shows the FFT of the circled area in the HRTEM image, which shows the diffraction spots corresponding to the [01$\bar{1}$] zone axis of monoclinic HfO_2. The values of interplanar distance d of pure HfO_2 film are about 0.5077 nm and 0.3640 nm corresponding to the (100) and (011) plane of the monoclinic phase (PDF-06-0318). While the HRTEM image of Y-doped HfO_2 (Y-9.2 mol%) reveals the (111) plane of the cubic phase with $d = 0.2987$ nm, and the inset shows the diffraction spots corresponding to the [10$\bar{1}$] zone near the axis of cubic HfO_2 (PDF-53-0560). The HRTEM analysis reveals that the pure HfO_2 film clearly crystallizes into monoclinic structure and transforms into the cubic phase with Y doping. Meanwhile, the results also confirm the identification of the process of phase change caused by Y doping in XRD patterns.

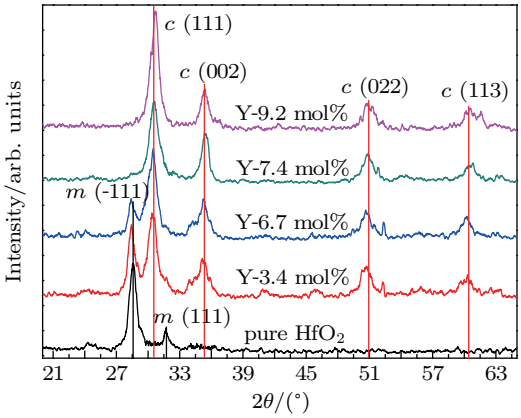


Fig. 4. (color online) X-ray diffraction patterns of films with different Y content values.

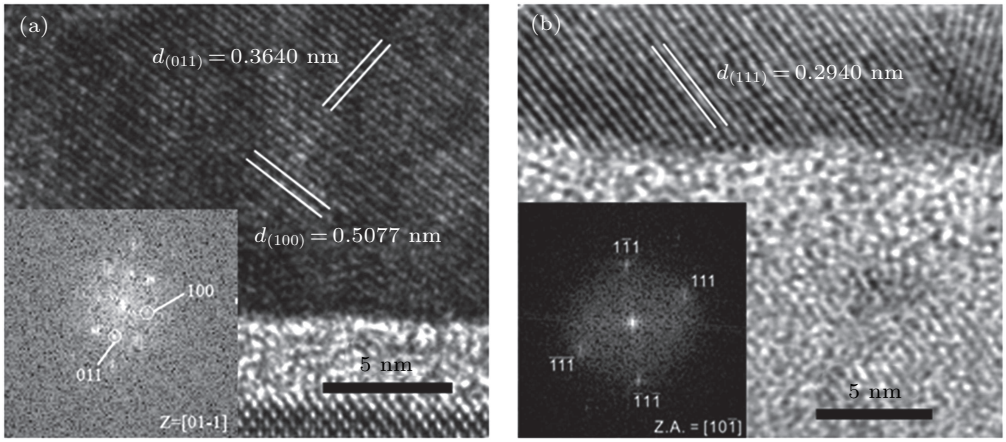


Fig. 5. HRTEM micrographs for HfO_2 films with different Y content: (a) pure HfO_2; (b) Y-9.2 mol%. Insets in panels (a) and (b) show selective area electron diffraction patterns.

3.3. Electrical properties

To understand the electrical properties of as-deposited HfO_2 films, electrical measurements are performed on MOS structures with top TiN electrodes. The leakage current densities measured as a function of applied voltage for different Y content are compared with that of a pure HfO_2 film in Fig. 6. The J–V measurements show that the leakage current density of pure deposited HfO_2 thin film is 1×10^{-5} A/cm^2 at 1 V. The leakage current density is observed to be improved significantly up to 1×10^{-6} A/cm^2 after the doping ratio of Y increases to 3.4 mol% in HfO_2 film. Since oxygen vacancies can be detected in insufficiently oxidized hafnia films containing less oxygen than stoichiometric HfO_2,[28] a number of oxygen vacancies exist in pure or Y-doped HfO_2 films in our case. Doping Y into HfO_2 can change the charged states of oxygen vacancies, which means that oxygen vacancies are passivated by Y.[29] This effect of Y doping can explain the reduction of leakage current density of Y-doped HfO_2, since oxygen va-

cancies would result in vacancy-mediated ionic conduction. However, the continuous increase of Y content does not significantly change the leakage current density. As a trivalent doping element, two Y atoms substituting for Hf sites results in a deficiency of two electrons, and this is compensated for by introducing an oxygen vacancy. Hence, a certain number of oxygen vacancies might be induced in the HfO_2 film with increasing Y content. The competition between these two effects results in the leakage current keeping unchanged as the Y content increases. This fact clearly shows that the Y-doped HfO_2 films have better leakage properties than pure HfO_2 films, and this advantage can be maintained until the single cubic HfO_2 phase is stabilized.

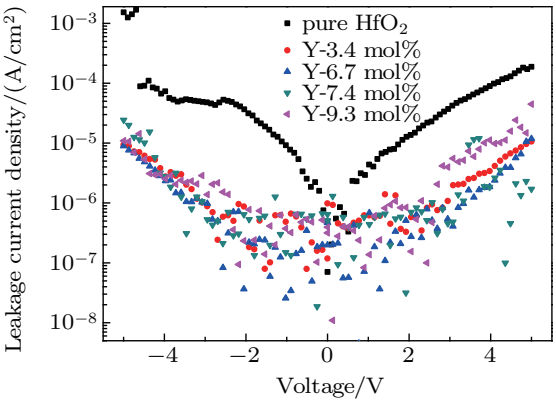


Fig. 6. (color online) Plots of leakage current density J versus applied voltage for Y-doped HfO_2 films grown on Si with different Y contents.

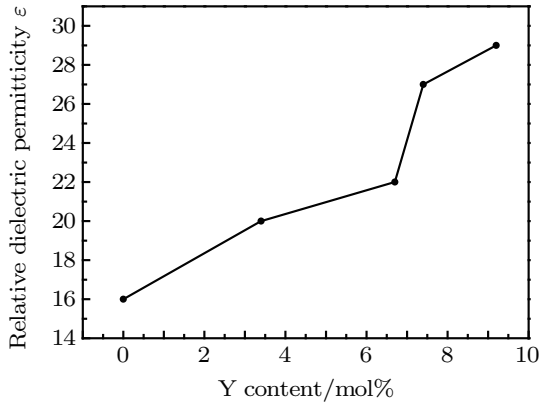


Fig. 7. Dielectric relative permittivity of the Y-doped HfO_2 film versus Y content.

The values of dielectric constant κ evaluated from TiN/Y-doped HfO_2/Si MOS structures with different Y contents are shown in Fig. 7, which clearly shows that Y-doping can increase κ of HfO_2 despite the fact that Y_2O_3 has a lower κ than HfO_2. The physical thickness of Y-doped HfO_2 film is strictly determined by HRTEM. When the doping ratio of Y increases to 7.4 mol%, the Y-doped HfO_2 shows a significant enhancement of κ (27) over pure HfO_2 (16). The abrupt increase of κ can be explained by the structural phase transformation from the monoclinic to the cubic by Y doping. The doping ratio of Y further increases to 9.2 mol%, resulting in a slight increase of κ (29). The slight increase of κ in the simple cubic HfO_2 film, perhaps, could be attributed to the preferred orientation of (111) plane.

4. Conclusions

In this work, the Y-doped HfO_2 thin films have been prepared by reaction magnetron sputtering deposition with Y content ranging from 0 mol% to 9.2 mol%. The effects of Y content on the composition, valence state, crystallographic structure, and dielectric properties of HfO_2 film are investigated. The XPS analyses indicate that the core levels of Hf 4f and O 1s shift to lower binding energy with Y content increasing, which is attributed to the difference in eletronegativity between cations. The surface of the sample is completely oxidized and the interfacial layer is mainly Hf silicate between Y-doped HfO_2 and Si. The analytical data of the crystal structure indicate that a constituent phase changes from low-permittivity monoclinic to high-permittivity cubic phase with the increase of Y content. A pure cubic phase is stabilized for Y content between 6.7 mol%–7.4 mol%, and the intensity of the peak at 30.7°, which corresponds to diffraction from (111) planes, increases with Y content increasing. The permittivity is found to be strongly dependent on the yttrium content, and its maximum is 29 for 9.2 mol%. The J–V curves show that the Y-doped HfO_2 films have better current leakage properties than pure HfO_2 films, which is attributed to the passivation of oxygen vacancies by dopant Y.

References

[1] Kingon A I Maria J P and Streiffer S K 2000 *Nature* **406** 1032
[2] Wilk G D, Wallace R M and Anthony J M 2001 *J. Appl. Phys.* **89** 5243
[3] Green M L, Gusev E P, Degraeve R and Garfunkel E 2001 *J. Appl. Phys. Rev.* **90** 2057
[4] Gaymax M, Van S E, Houssa M, Delabie A, Conard T, Meuris M, Heyns M M, Dimoulas A, Spiga S, Fanciulli M, Seo J W and Goncharova L V 2006 *Mater. Sci. Eng. B* **135** 256
[5] Lee B H, Kang L, Qi W J, Nieh R, Jeon Y, Onishi K and Lee J C 1999 *Tech. Dig. IDEM* **99** 133
[6] Robertson 2000 *J. Vac. Sci. Technol. B* **18** 1785
[7] Wilk G D, Wallace R M and Anthony J M 2001 *J. Appl. Phys.* **89** 5243
[8] Torchio P, Gatto A, Alvisi M, Albrand G, Kaiser N and Amra C 2002 *Appl. Opt.* **41** 3256
[9] Miyata N, Yasuda T and Abe Y 2010 *J. Appl. Phys.* **107** 103536
[10] Cho J, Nguyen V, Ritcher C A, Ehrstein R, Lee B H and Lee J C 2002 *Appl. Phys. Lett.* **80** 1249
[11] Hsieh C R, Chen Y Y and Lou J C 2010 *Appl. Phys. Lett.* **96** 022905
[12] Villanueva-lbańez M, Luyer L C, Parola S, Matry O and Mugnier Mugnier J 2003 *Rev. Adv. Mater. Sci.* **5** 296
[13] Ferrari S, Modreanu M, Scarel G and Fancinelli M 2004 *Thin Solid Films* **450** 124
[14] Tang J, Zhang F, Zoogman P, Fabbri J, Chan S W, Zhu Y, Brus L E and Steigerwald M L 2005 *Adv. Funct. Mater.* **15** 1595
[15] Noor-a-Alam M, Abhilash K and Ramana C V 2012 *Thin Solid Films* **520** 6631

[16] Kita K, Kyuno K and Toriumi A 2005 *Appl. Phys. Lett.* **86** 102906
[17] Xie Y, Ma Z, Su Y, Liu Y, Liu L, Zhao H, Zhou J, Zhang Z, Li J and Xie E 2011 *J. Mater. Res.* **26** 50
[18] Frandons J, Broussrau B and Pradal F 1980 *Phys. Stat. Sol. B* **98** 379
[19] Han Kai, Wang Xiao-Lei, Yang Hong and Wang Wen-Wu 2013 *Chin. Phys. B* **22** 117701
[20] Meng Yong-Qiang, Liu Zheng-Tang, Feng Li-Ping and Cheng Shuai 2014 *Chin. Phys. Lett.* **31** 077702
[21] Ma X L, Yang H, Xiang J J, Wang X L, Wang W W, Zhang J Q, Yin H X, Zhu H L and Zhao C 2017 *Chin. Phys. B* **26** 027701
[22] Kadlec F and Simon P 2000 *Mater. Sci. Eng. B* **72** 56
[23] Duwez P, Brown F H and Odell F 1951 *J. Electrochem. Soc.* **98** 356
[24] Chen X Y, Song L X, You L J and Zhao L L 2013 *Appl. Surf. Sci.* **271** 248
[25] Wong H, Zhan N, Ng K L, Poon M C and Kok C W 2004 *Thin Solid Films* **462–463** 96
[26] Tan R, Azuma Y and Kojima I 2005 *Appl. Surf. Sci.* **241** 135
[27] Lee C K, Cho E, Lee H S, Hwang C S and Han S 2008 *Phys. Rev. B* **78** 012102
[28] Takeuchi H, Ha D and King T J 2004 *J. Vac. Sci. Technol. A* **22** 1337
[29] Chen G H, Hou Z F, Gong X G and Li Q 2008 *J. Appl. Phys.* **104** 074101